ACS APPLIED MATERIALS & INTERFACES

Research Article

www.acsami.org

Hollow Mesoporous Silica Nanoparticles with Tunable Structures for Controlled Drug Delivery

Yanhua Li,[†] Na Li,[†] Wei Pan, Zhengze Yu, Limin Yang, and Bo Tang*

College of Chemistry, Chemical Engineering and Materials Science, Collaborative Innovation Center of Functionalized Probes for Chemical Imaging in Universities of Shandong, Key Laboratory of Molecular and Nano Probes, Ministry of Education, Institute of Molecular and Nano Science, Shandong Normal University, Jinan 250014, P.R. China

Supporting Information

ABSTRACT: A size-controllable and facile synthetic strategy has been developed to fabricate a series of hollow mesoporous silica nanoparticles (HMSNs) with tunable hollow cores or shell thicknesses by employing gold nanoparticles (Au NPs) and cetyltrimethylammonium bromide (CTAB) as dual templates. Various sizes of Au NPs and different amounts of tetraethyl orthosilicate contributed to structure-tailored mesoporous silica-coated Au NPs. After calcination, CTAB molecules were completely removed, and Au NPs could still support the silica shell due to the high melting point. HMSNs were ultimately obtained by etching Au NPs. Applications of HMSNs as nanocarriers for delivering drugs were investigated. Significantly, it was flexible and convenient to control drug-loading/releasing behavior of HMSNs just by tuning the hollow cores or shell thicknesses. Intracellular experiments have proven that HMSNs are suitable for delivering drugs. We anticipate that this study could provide an important avenue for the synthesis of HMSNs and further contribute to advancing practical applications of HMSNs in drug delivery systems.

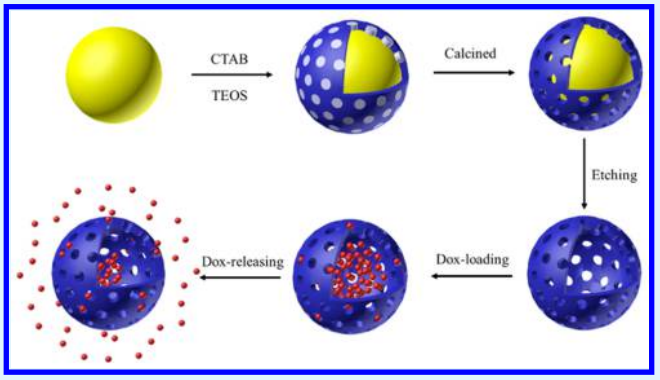

KEYWORDS: *hollow mesoporous silica nanoparticles, Au NPs, hollow cavity, shell thickness, drug-loading, drug-releasing*

INTRODUCTION

Conventional drugs generally have many nonideal properties, such as poor solubility, unexpected biodistribution, and premature degradation, that seriously affect their potency during the therapeutic process.[1] Drug delivery systems have attracted significant interest because they can improve many pharmacological properties of free drugs.[1] Ideal drug delivery systems should possess the following features: good biocompatibility, protection of the drugs, high loading and controllable release of the drugs, efficient cellular uptake, and so forth.[2−5] Nanocarriers always provide significant merits as drug delivery systems, including the fact that (i) nanocarriers are nanoscale materials that can easily enter cells in abnormal tissues, (ii) each nanomaterial can carry thousands of drug molecules, thus increasing the intracellular concentration of the drugs, and (iii) nanocarriers can also be supposed to control the release of drugs as required to ensure the potency of the drug.[6−14] Among diversified nanocarriers, mesoporous silica nanoparticles (MSNs) have attracted significant attention on account of their regular structural characteristics, great surface areas, tunable pore diameters, good thermal and chemical stabilities, excellent biocompatibility, and ease of surface modification.[8−12] Therefore, MSNs have been designed as nanocarriers for delivery of disparate cargoes into cancer cells, especially hydrophilic or hydrophobic anticancer drugs.[15−17] With advances in the fields of biotechnology and nanomedicine, MSNs cannot satisfy the extension of applications in biomedical research due to their limited loading capacity. Hence, many attempts are ongoing to optimize the structure of MSNs to exploit their application areas.[18] For incorporating the advantages of MSNs and microsphere capsules into drug carriers, the synthesis of HMSNs has been proposed. MSNs with rattle or hollow structure must be particularly noteworthy in drug delivery systems because they can efficiently accommodate drugs into not only mesoporous channels but also the hollow interiors.[19,20]

HMSNs with unique large hollow cavities, intact porous shells, and well-defined and controllable particle morphologies, have great potential in diverse applications: (i) The interstitial hollow cavities can serve as reservoirs to store cargo or as nanoreactors to support chemical reactions. (ii) Mesopores enable the cargo to diffuse through the intact shell. (iii) Abundant Si−OH bonds on the silica surface are flexible enough to be modified by various chemicals for potential applications.[21,22] Template-eliminated methods, such as soft- and hard-templating methods, were the most commonly used synthetic strategies for fabricating HMSNs, which mainly consist of two steps: formation of the core−shell structure and subsequent removal of the cores.[21,22] However, there are still problems that require

Received: October 30, 2016
Accepted: December 22, 2016
Published: December 22, 2016

© 2016 American Chemical Society

DOI: 10.1021/acsami.6b13876
ACS Appl. Mater. Interfaces 2017, 9, 2123−2129

Scheme 1. Schematic Illustration for the Preparation of HMSNs and Their Use in Drug Loading and Release

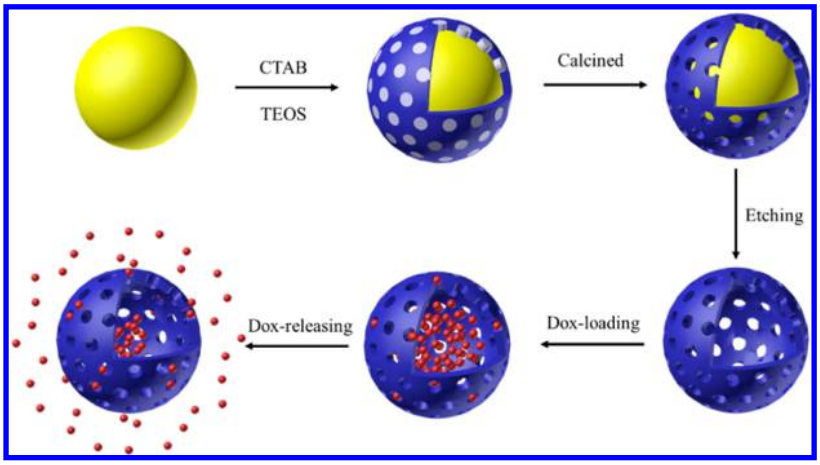

urgent resolution in conventional template-eliminated methods. Soft templates, such as emulsion droplets, gas bubbles, and supramolecular micelles/vesicles, generally represent low structural stability and poor uniformity in solution; the obtained hollow materials are often not controllable in morphology and size distribution. In addition, the thickness of shell and the size of hollow core cannot be flexibly and independently controlled by these techniques.[23] As for using an organic polymer as a hard template, the core−shell particles generally undergo high-temperature calcination or washing by specific organic reagents for removal of templates and surfactant, resulting in open mesopores and hollow cavities.[24] However, as the core templates and surfactant cleared at the same time, the obtained hollow cavities will inevitably collapse because of the lack of support from the core templates, and yet, washing by organic reagents cannot remove the templates completely and will inevitably lead to a residue of CTAB, which will further cause cytotoxicity.

Herein, we report a clear, flexible, and size-controllable synthetic strategy to fabricate the HMSNs with tunable hollow cores and mesoporous shells. We introduced gold nanoparticles (Au NPs) as the hard template and cetyltrimethylammonium bromide (CTAB) as the mesoporous template agents during the synthesis process. The narrow size distribution and tunable diameter of Au NPs[25] made it easy to tune the size of hollow cores. CTAB acts not merely as a stabilizing cationic surfactant for the cores but also as the common organic mesoporous template agent for forming mesoporous silica shells in the synthesis process.[26] For the CTAB molecules to be removed completely the core−shell nanoparticles were calcined in air at 450 °C. On account of the high melting point of the Au NPs, they still support the mesoporous silica shell even at high temperature. Thus, this step can not only achieve complete removal of CTAB but also maintain the integrity of mesoporous silica shells. After removal of CTAB, the HMSNs were finally obtained by etching the Au NPs. The uniform and structure-tailored HMSNs were employed as the nanocarrier for anticancer drug delivery. Significantly, it was flexible and convenient to control the drug-loading and -releasing behavior of HMSNs just by tuning the size of the hollow cores or shell thicknesses. Details of this process are presented in Scheme 1.

EXPERIMENTAL SECTION

Reagents and Materials. Sodium borohydride ($NaBH_4$), cetyltrimethylammonium bromide (CTAB), trisodium citrate dihydrate ($C_6H_5Na_3O_7{\cdot}2H_2O$), ascorbic acid, hydrogen peroxide (H_2O_2, 30%), tetraethyl orthosilicate (TEOS), and hydrogen tetrachloroaurate (III) ($HAuCl_4{\cdot}4H_2O$, 99.99%) were purchased from China National Pharmaceutical Group Corporation (Shanghai, China). Thiourea was purchased from BO DI Chemical Ind., Co., Ltd. (Tianjin, China). Doxorubicin hydrochloride (Dox) was purchased from Sangon Biotechnology Co., Ltd. (Shanghai, China). 3-(4,5-Dimethyl-thiazol-2-yl)-2,5-diphenyltetrazolium bromide (MTT) was purchased from Sigma Chemical Company. All the chemicals were of analytical grade and used without further purification. Sartorius ultrapure water (18.2 MΩ cm) was used throughout the experiments. The human breast cancer cell line MCF-7 was purchased from KeyGEN Biotechnology Company (Nanjing, China).

Apparatus. Transmission electron microscopy (TEM) was carried out on a JEM-100CX Π electron microscope. Fluorescence spectra were obtained with an FLS-920 Edinburgh Fluorescence Spectrometer with a xenon lamp and 1.0 cm quartz cells at slits of 1.5/1.5 nm. All pH measurements were performed with a pH-3c digital pH meter (Shanghai LeiCi Device Works, Shanghai, China) with a combined glass-calomel electrode. Absorbance was measured in a microplate reader (Synergy 2, Biotek, USA) in the MTT assay. Confocal fluorescence imaging studies were performed with a TCS SP5 confocal laser scanning microscope (Leica Co., Ltd. Germany) with a 40× objective lens.

Preparation of Au NPs with Different Sizes. Gold nanoparticles (Au NPs) with various sizes were synthesized using a seed-mediated growth procedure according to a reported protocol with some modifications.[27] Twenty microliters of aqueous solution with 0.25 mM $HAuCl_4$ and 0.25 mM trisodium citrate was prepared first. Then, 600 μL of cold and fresh $NaBH_4$ solution (0.1 M) was added to the above mixture, which resulted in the formation of a pink solution. The seed solution was stirred vigorously for 1 min and then kept at 25 °C for another 2 h for further use.

The growth solution was prepared as follows. First, 200 mL of aqueous solution containing $HAuCl_4$ (final concentration of 0.25 mM) was prepared. Then, 6 g of CTAB (final concentration of 0.08 M) was added to the solution with gentle stirring at 45 °C until the mixture turned clear orange. The solution was kept at 25 °C as a stock growth solution.

Then, 100 μL of 0.1 M ascorbic acid solution was added to 18 mL of growth solution, which resulted in the formation of a clear colorless solution; 2 mL of seed solution was then added with vigorous stirring for 10 min. The as-prepared particles (~8 nm, designated as set A) were kept at 25 °C for 30 min and then used as the seeds for preparing Au NPs of 15 nm (set B). Similarly, Au NPs of 30, 40, and 50 nm were prepared using different volumes of set B as the seeds.

Preparation of Au NPs@MS. Mesoporous silica-coated Au NPs (Au NPs@MS) were synthesized as follows.[28,29] The as-synthesized Au NPs were centrifuged to remove excess CTAB and redispersed in 20 mL of water. Eight milliliters of ethanol and 400 μL of NaOH (0.1 M) were added to the Au NPs as described above.

DOI: 10.1021/acsami.6b13876
ACS Appl. Mater. Interfaces 2017, 9, 2123−2129

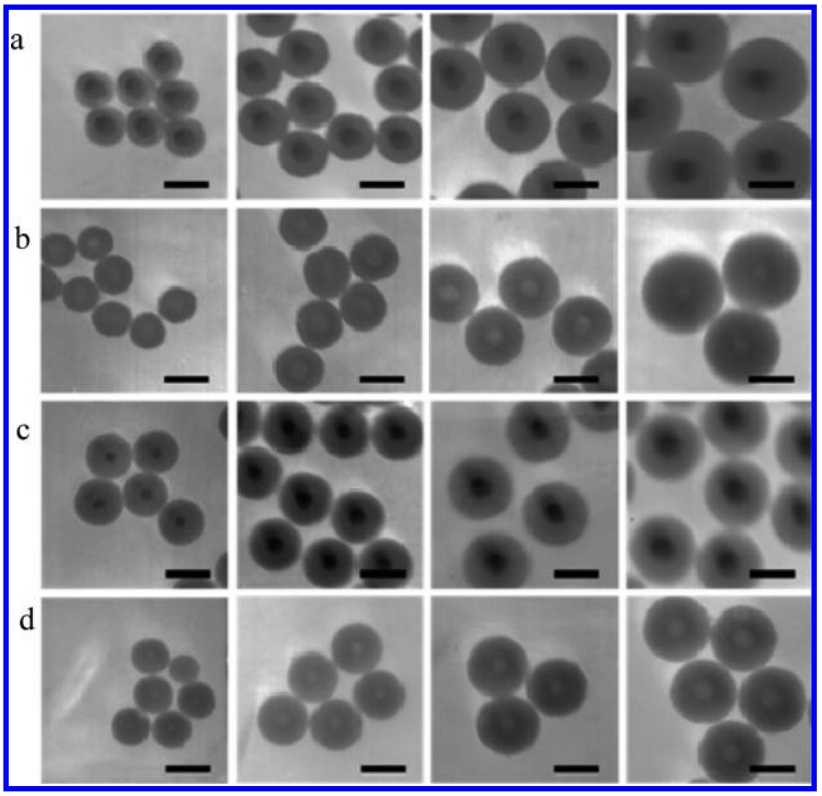

Figure 1. TEM images of Au NPs@MS with different shell thicknesses of 20, 30, 45, and 70 nm (a) and Au NPs@MS with different core sizes of 15, 30, 40, and 50 nm (c). TEM images of HMSNs with various shell thicknesses of C50−S20, C50−S30, C50−S45, and C50−S70 (b) and HMSNs with various hollow core sizes of C15−S45, C30−S45, C40−S45, and C50−S45 (d). Scale bars are 100 nm.

The mixture was gently stirred for 10 min. Then, different volumes (80−160 μL) of 5% TEOS (0.5 mL of TEOS dispersed in 10 mL of ethanol) were added three times under gentle stirring at 30 min intervals. The mixture reacted for 24 h at 30 °C to form the mesoporous silica shell with various thicknesses. A part of as-synthesized Au NPs@MS was washed with ethanol and water several times, and we called it Au NPs@MS (washing). The rest of Au NPs@MS was then calcined at 450 °C for 10 h to remove the CTAB remaining inside the mesopores, and we called it Au NPs@MS (calcination). The two kinds of Au NPs@MS were used to prepare various hollow mesoporous silica nanoparticles, designated as HMSNs (washing) and HMSNs (calcination), respectively.

Preparation of HMSNs. Hollow mesoporous silica nanoparticles (HMSNs) were obtained by etching the gold cores of Au NPs@MS. One millliliter of thiourea solution (1 M, pH 2.0, H_2SO_4) was mixed with 0.5 mL of enriched Au NPs@MS solution. After 30 min, 50 μL of H_2O_2 (1 M) was added to the mixed solution, which resulted in the complete dissolution of gold cores within 5 min. The suspension was then centrifuged and washed several times. HMSNs were dried and weighed for further use.

Preparation of MSNs. Mesoporous silica nanoparticles (MSNs) were prepared via the previously reported method with a few modifications.[30,31] First, 240 mL of aqueous solution containing 0.5 g of CTAB was prepared in a conical flask. Then, 1.5 mL of NaOH (aq) (2 M) was added to the above-mentioned solution with stirring for 10 min. After the temperature of the mixture was adjusted to 80 °C, 2.5 mL of TEOS was added dropwise to the solution. MSNs were produced after stirring for 2 h. The as-prepared MSNs were centrifuged and washed with ethanol and deionized water several times to remove the surfactant template and then dried in air for further use. We called them MSNs (washing). For CTAB to be completely removed, the precipitates were calcined at 450 °C for 10 h. We called them MSNs (calcination).

Preparation of HMSNs(Dox) and MSNs(Dox). First, 2 mg/mL of HMSNs was mixed with 0.8 mg/mL of Dox. This mixture was kept stirring for at least 24 h in darkness to achieve the largest loading of Dox. Then, 100 μL of the solution was centrifuged (10000 rpm, 10 min), and the supernatant was discarded. The precipitates, designated as HMSNs(Dox), were redispersed in 1 mL of deionized water for further use. The preparation of MSNs(Dox) was same as the method described above.

Quantitation of Dox Loaded into the Nanocarrier. For the Dox molecules that were loaded into the nanocarrier to be quantified, 1 mL of HMSNs(Dox) or MSNs(Dox) solution was heated at 80 °C for at least 30 min. After centrifugation, the supernate of the sample was separated, and the precipitates were redispersed in 1 mL of deionized water. For ensuring thorough Dox molecule release from the pores of the nanocarrier, the above process was repeated at least two times. The fluorescence intensity (λ_{ex} = 490 nm, λ_{em} = 590 nm) of the supernate was obtained with an FLS-920 Edinburgh Fluorescence Spectrometer, and the concentrations of Dox were in proportion to the fluorescence intensity in Standard linear calibration curve of Dox (Figure S1). The drug loading content = mass of drugs in the HMSN/mass of the drug-loaded HMSN. The loading content of Dox was calculated to be 0.099 mg of Dox per 1 mg of HMSNs:C50−S20. The loading capacities of various materials were measured the same way as the above, and the results are shown in Table S1.

Dox Release of HMSNs(Dox). A series of Dox-loaded HMSNs were respectively dispersed in 2 mL of PBS (pH 5.0) and stored at room temperature. The fluorescence intensities of the samples were measured (λ_{ex} = 490 nm, λ_{em} = 590 nm) at different time periods. The experiment was repeated three times, and the data are shown as the mean ± SD.

Confocal Fluorescence Imaging. HMSNs(Dox) and MSNs(Dox) (0.1 mg/mL) were respectively delivered into the MCF-7 cells (cultured at 37 °C in 5% CO_2) in DMEM culture medium for 2 h. Then, cells were examined by confocal laser scanning microscopy with 488 nm excitation after being washed three times with PBS buffer. The cell nuclei were counterstained by Hoechst 33342.

DOI: 10.1021/acsami.6b13876
ACS Appl. Mater. Interfaces 2017, 9, 2123−2129

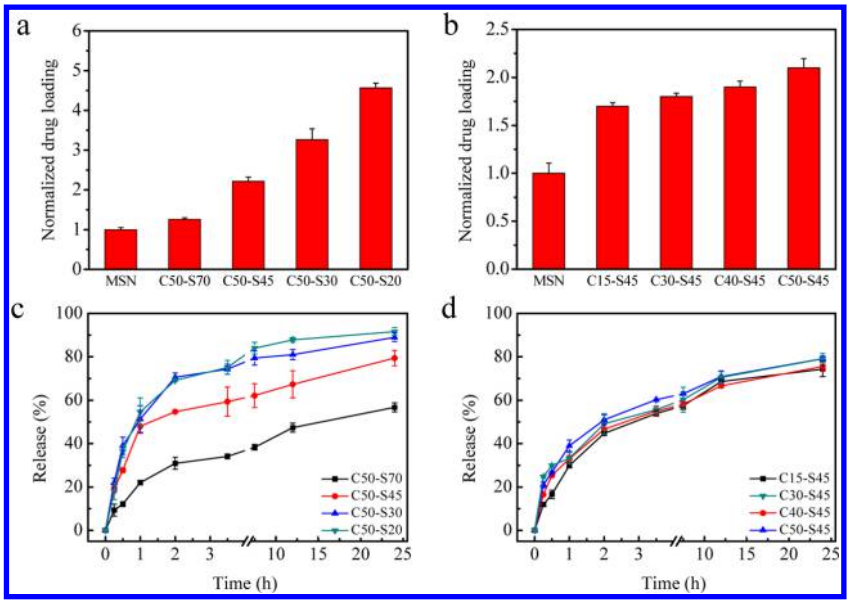

Figure 2. Dox loading capability of MSNs (normalized to 1) as well as HMSNs with different shell thicknesses (a) and various sizes of hollow cores (b) with ratios of 1:1.3:2.2:3.3:4.6 and 1:1.7:1.8:1.9:2.1, respectively. Percentage of Dox released from HMSNs with different shell thicknesses (c) and various sizes of hollow cores (d) (n = 3, mean ± SD).

MTT Assay. The cytotoxicity of the nanocarriers was determined by MTT assay[32] in MCF-7 cells. MCF-7 cells (5000 cells/well) in 96-well microtiter plates were respectively incubated with HMSNs(W), MSNs(W), HMSNs(C), and MSNs(C) (0.1 mg/mL) dissolved in DMEM culture medium for 6 h. Cells were washed with PBS three times and cultured with DMEM at 37 °C for another 24 h. Then, MTT solution (150 μL, 0.5 mg/mL in PBS) was added to each well. After 4 h, the MTT solution remaining in each well was removed, and 150 μL of DMSO was added to dissolve the formazan crystals. The absorbance of formazan crystals in DMSO was measured with a microplate reader at 490 nm. Cells incubated without nanocarrier served as the control. The experiment was repeated three times, and the data are shown as the mean ± SD.

For the therapeutic effects of the drugs loaded in HMSNs and MSNs to be compared, MCF-7 cells were respectively incubated with HMSNs(Dox) and MSNs(Dox) (0.1 mg/mL) dissolved in DMEM culture medium for 6 h. Then, the cells were washed with PBS three times. After that, cells were cultured with DMEM at 37 °C for another 24 h. Next, the absorbance of the formazan crystals in DMSO was measured with the same method as mentioned above. Cells incubated without nanocarrier served as the control. The experiment was repeated three times, and the data are shown as the mean ± SD.

RESULTS AND DISCUSSION

Synthesis and Characterization of HMSNs and MSNs. The Au NPs were first prepared via the seed-mediated growth process in accordance with the previously reported method with some improvements.[27] The use of Au NPs as core templates has two advantages: one is their narrow size distribution, tunable diameter, uniform spherical morphology, and good dispersibility, and the other is their high melting point. The sizes of the Au NPs can be precisely controlled from 15 to 50 nm by tuning the seed solution. Then, the core−shell nanoparticles with Au NPs as cores and mesoporous silica as shells (designated as Au NPs@MS) were prepared by the sol−gel reaction.[28,29] CTAB, a positively charged agent, is not merely used as stabilizing cationic surfactant for Au NPs but also as an organic template for building mesoporous silica shells.[26,33,34] However, the cationic surfactant CTAB is cytotoxic and can prevent the positively charged drug, doxorubicin (Dox), from loading into te mesoporous silica shell by the electrostatic interaction; thus, it is significant to completely remove the CTAB templates. As can be seen in Figure 1a and c, the Au NPs@MS with different core sizes or shell thicknesses are monodisperse and precisely size-controllable. Upon calcination of the Au NPs@MS in air at 450 °C for 10 h to remove CTAB templates, the resulting Au NPs@MS exhibited microsphere morphology with diameters the same as before. The analysis of constant elements indicated that there was no residual carbon and nitrogen, which indicated that CTAB templates were removed completely (Table S2). Then, the HMSNs were obtained by etching gold cores from the as-synthesized Au NPs@MS. The technique is highly flexible for controlling the structure of HMSNs: the diameters of cavities can be tuned from 15 to 50 nm and the shell thicknesses from 20 to 70 nm. The monodispersed HMSNs with uniform hollow cores of 50 nm and different shell thicknesses of 20, 30, 45, and 70 nm (designated as HMSNs: C50−S20, C50−S30, C50−S45, C50−S70, respectively) as well as hollow cores of 15, 30, 40, and 50 nm and similar shell thickness of 45 nm (designated as HMSNs: C15−S45, C30−S45, C40−S45, C50−S45, respectively) are shown in Figure 1b and d.

Nitrogen adsorption−desorption isotherms of HMSNs were recorded to investigate the surface area and porosity of the materials. As can be seen in Figure S2, N_2 adsorption−desorption isotherms of HMSNs, C50−S20, C50−S45, C50−S70, and C15−S45, showed typical Type IV curves. The high N_2 uptake below a pressure of 0.1 clearly indicates that massive micropores are present. Calculated by the Barrett−Joyner−Halenda (BJH) method, the pore sizes centered around 0.65, 0.65, 0.61, 0.63 nm, respectively (inset in Figure S2). The Brunauer−Emmett−Teller (BET) surface areas are 1047, 959, 735, and 955 $m^2\ g^{-1}$, respectively. After loading with Dox, the surface areas of HMSNs, C50−S20, C50−S45, C50−S70, and C15−S45, become 624, 877, 575, and 731 $m^2\ g^{-1}$, respectively, which further confirms that the drugs have been loaded into the nanoparticles (Table S3).

DOI: 10.1021/acsami.6b13876
ACS Appl. Mater. Interfaces 2017, 9, 2123−2129

In the control, a portion of the Au NPs@MS was first subject to etching and then calcination in air at 450 °C for 10 h, which resulted in an absolute framework collapse of the HMSNs due to the lack of support from Au NPs at high temperature (Figure S3). For the effect of residual CTAB in mesopores on the drug loading of HMSNs to be demonstrated, another HMSN was prepared as a control by washing with ethanol and deionized water several times to remove the CTAB templates (designated as HMSNs(W)). Figure S4 indicates that the HMSNs prepared by calcination (designated as HMSNs(C)) show better capacity for drug loading compared to that of HMSNs(W). As a consequence, that residual CTAB can prevent the positively charged drugs from loading into HMSNs was further proven. Mesoporous silica nanoparticles (MSNs) were prepared as the control. As can be seen from the TEM image of MSNs in Figure S5, the prepared MSNs are spherical and monodisperse.

Drug-Loading/Releasing Behavior of Various HMSNs. For further application of HMSNs as nanocarriers, various HMSNs were loaded with Dox to evaluate the effect of mesoporous shell thicknesses and the sizes of hollow cores on drug-loading and -releasing behavior. By contrast, MSNs were prepared via the reported procedure.[30,31] As shown in Figure 2a and b, the drug-loading capacity of HMSNs is higher than that of MSNs. Most significantly, the drug-loading capacity of HMSNs with uniform hollow cores increases along with the decreasing thicknesses of the shell (Figure 2a), and the loading capacity of HMSNs with the same shell thickness increases along with the increasing sizes of cavities (Figure 2b). Obviously, Dox molecules are entrapped in both the cavities and the mesoporous shells. Then, the drug-releasing behavior of Dox-loaded HMSNs (designated as HMSNs(Dox)) with various shell thicknesses or different sizes of hollow cores was investigated. As can be seen in Figure 2c and d, all systems exhibit a small burst-release of Dox molecules from HMSNs in the first hour. After that, the rest of the cargo molecules show a relatively slow release rate. Figure 2c shows that the HMSNs with uniform hollow cores and various shell thicknesses give rise to different release rates and amounts of Dox. After 24 h of release, the amounts of released Dox reach 56.7% for C50−S70, 79.4% for C50−S45, 89.0% for C50−S30, and 91.6% for C50−S20. Both release rates and amounts of Dox from HMSNs C50−S20 and C50−S30 present similar trends, which indicates that the shell thickness of 30 nm is too thin to limit the diffusion of the cargo molecules from HMSNs.

For the HMSNs with uniform shell thickness and various diameters of hollow cores, the release rates and amounts of Dox do not show discernible change (Figure 2d), which indicates that the shell thicknesses have a dominant influence on drug-release behavior of the HMSNs(Dox). Consequently, it is more practical and flexible to control the drug-releasing behavior of HMSNs(Dox) just by tuning the thicknesses of the mesoporous shell. Figure S6 shows that the drug-release behavior here can be analyzed using the Higuchi model, which verifies that the drug-releasing behavior of HMSNs(Dox) is consistent with the Fickian diffusion mechanism.[35] According to this model, the amount of released drugs exhibits a linear relationship if plotted against the square root of time, which illustrates that it is a purely diffusion-controlled process.[36] It further indicates that the drug-release behavior of the HMSNs(Dox) is affected by the shell thicknesses.

Confocal Fluorescence Imaging in Living Cells. For HMSNs to be utilized for drug delivery in practical applications, intracellular experiments were implemented with the human breast cancer cell line MCF-7. As can be seen in Figure 3, negligible intracellular background fluorescence signal was observed

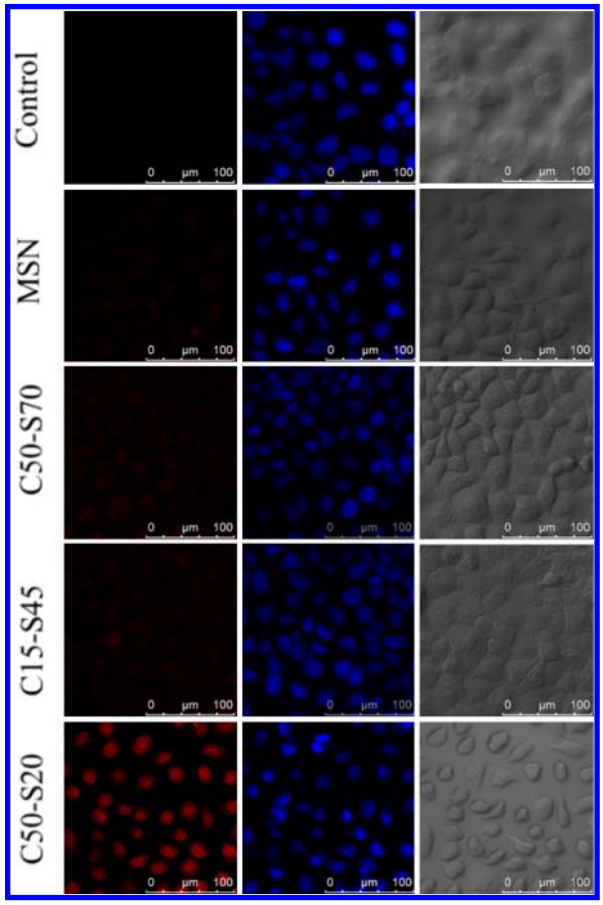

Figure 3. Confocal fluorescence images: dark-field images (left), cell nucleus counterstained by Hochest (middle), bright-field images (right) of MCF-7 cells after incubation with only DMEM culture medium (control), MSNs(Dox), and HMSNs C50−S70(Dox), C15−S45(Dox), and C50−S20(Dox) (0.1 mg/mL). Scale bars are 100 μm.

under confocal laser scanning microscopy. Slightly enhanced fluorescence was observed after incubating MCF-7 cells with MSNs(Dox) compared to that of the control, and cells with HMSNs C50−S70(Dox) and C15−S45(Dox) showed slightly stronger fluorescence signals. When MCF-7 cells were incubated with the HMSNs C50−S20(Dox), the fluorescence intensity is much higher (Figure 3). The fluorescence intensities of cells were consistent with those of the drug-loading/releasing experiment. Bright-field images in Figure 3 (right) indicate that the MCF-7 cells were viable in the intracellular experiments. As can be seen in Figure S7, the average fluorescence intensity of cells was also measured, which further confirmed that the HMSNs C50−S20(Dox) showed better drug delivery capacity than HMSNs C50−S70(Dox) and C15−S45(Dox), and MSNs.

Cytotoxicity Assay. MTT assays were carried out in MCF-7 cells to evaluate the in vitro cytotoxicity of HMSNs. MCF-7 cells incubated without any nanocarrier served as the control. Figure 4a shows that the cell viability was more than 95% when MCF-7 cells were incubated with the HMSNs(C) or MSNs(C), respectively, whereas only 86 and 72% survived when MCF-7 cells were incubated with the HMSNs(W) or MSNs(W), respectively. This further proves that the residual

DOI: 10.1021/acsami.6b13876
ACS Appl. Mater. Interfaces 2017, 9, 2123−2129

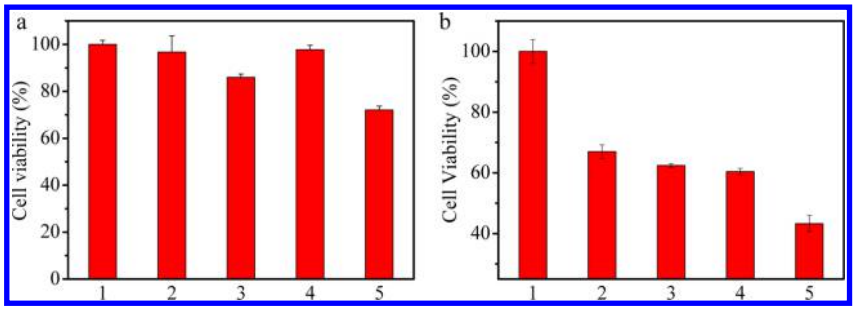

Figure 4. MTT assay of MCF-7 cells. (a) 1, control (cells incubated without any nanocarriers); 2, HMSNs(C); 3, HMSNs(W); 4, MSNs(C); 5, MSNs(W) (0.1 mg/mL); (b) 1, control (cells incubated without any nanocarriers); 2, MSNs(Dox); 3, C50−S70(Dox); 4, C15−S45(Dox); 5, C50−S20(Dox) (0.1 mg/mL) for 6 h and then cultured with DMEM for 24 h at 37 °C (n = 3, mean ± SD).

CTAB molecules are cytotoxic, which are supposed to be completely removed from mesopores by calcination. For the potential application of HMSNs in the drug delivery system, Dox molecules were loaded to investigate the therapeutic effect of HMSNs(Dox). The viability of cells decreased successively when they were incubated with MSNs(Dox), C50−S70(Dox), C15−S45(Dox), and C50−S20(Dox) (Figure 4b). The result is consistent with that of the drug-loading/releasing experiment and intracellular imaging, which further confirms that the HMSNs can be used as an outstanding nanocarrier for drug delivery.

CONCLUSIONS

In summary, HMSNs with tunable hollow sizes and shell thicknesses were successfully synthesized by a controllable and facile synthetic strategy by using Au NPs and CTAB as dual templates. Different ways of removing the CTAB template had a significant influence on the cytotoxicity of as-prepared HMSNs. Moreover, the hollow core diameter and shell thickness had a significant impact on the drug-loading/releasing behavior of HMSNs. Experimental results indicated that the drug-releasing behavior of HMSNs(Dox) was consistent with the Fickian diffusion mechanism. Results of confocal fluorescence imaging and MTT assays further verified HMSNs as well-behaved drug carriers. We project that this strategy could provide an important avenue for synthesis of HMSNs, and this study may contribute to advancing the practical application of HMSNs in drug delivery systems.

ASSOCIATED CONTENT

Supporting Information

The Supporting Information is available free of charge on the ACS Publications website at DOI: 10.1021/acsami.6b13876.

Elemental analysis, TEM images, and other materials characterization (PDF)

AUTHOR INFORMATION

Corresponding Author

*E-mail: tangb@sdnu.edu.cn.

ORCID

Bo Tang: 0000-0002-8712-7025

Author Contributions

†Y.L. and N.L. contributed equally to this work.

Notes

The authors declare no competing financial interest.

ACKNOWLEDGMENTS

This work was supported by 973 Program (2013CB933800), the National Natural Science Foundation of China (21390411, 21535004, 21422505, 21375081, 21505087), and the Natural Science Foundation for Distinguished Young Scholars of Shandong Province (JQ201503).

ABBREVIATIONS

HMSNs = hollow mesoporous silica nanoparticles
AuNPs = gold nanoparticles
CTAB = cetyltrimethylammonium bromide
TEOS = tetraethyl orthosilicate
AuNPs@MS = mesoporous silica-coated AuNPs
HMSNs(W) = HMSNs (washing)
HMSNs(C) = HMSNs (calcination)
MSNs(W) = MSNs (washing)
MSNs(C) = MSNs (calcination)
HMSNs(Dox) = Dox loaded into HMSNs
MSNs(Dox) = Dox loaded into MSNs
MCF-7 cells = human breast cancer cell line
MTT = 3-(4,5-dimethyl-thiazol-2-yl)-2,5-diphenyltetrazolium bromide

REFERENCES

(1) Allen, T. M.; Cullis, P. R. Drug Delivery Systems: Entering the Mainstream. *Science* **2004**, *303*, 1818−1822.
(2) Vivero-Escoto, J. L.; Slowing, I. I.; Trewyn, B. G.; Lin, V. S. Y. Mesoporous Silica Nanoparticles for Intracellular Controlled Drug Delivery. *Small* **2010**, *6*, 1952−1967.
(3) Raeesi, V.; Chou, L. Y. T.; Chan, W.C. W. Tuning the Drug Loading and Release of DNA-Assembled Gold-Nanorod Superstructures. *Adv. Mater.* **2016**, *28*, 8511−8518.
(4) Wei, M.; Chen, N.; Li, J.; Yin, M.; Liang, L.; He, Y.; Song, H.; Fan, C.; Huang, Q. Polyvalent Immunostimulatory Nanoagents with Self-Assembled CpG Oligonucleotide-Conjugated Gold Nanoparticles. *Angew. Chem., Int. Ed.* **2012**, *51*, 1202−1206.
(5) Li, J.; Pei, H.; Zhu, B.; Liang, L.; Wei, M.; He, Y.; Chen, N.; Li, D.; Huang, Q.; Fan, C. Self-Assembled Multivalent DNA Nanostructures for Noninvasive Intracellular Delivery of Immunostimulatory CpG Oligonucleotides. *ACS Nano* **2011**, *5*, 8783−8789.
(6) Peer, D.; Karp, J. M.; Hong, S.; Farokhzad, O.; Margalit, R.; Langer, R. Nanocarriers as an Emerging Platform for Cancer Therapy. *Nat. Nanotechnol.* **2007**, *2*, 751−760.
(7) Singh, M. N.; Hemant, K. S. Y.; Ram, M.; Shivakumar, H. G. Microencapsulation: a Promising Technique for Controlled Drug Delivery. *Res. Pharm. Sci.* **2010**, *5*, 65−77.
(8) Chang, Y.; Liao, P.; Sheu, H.; Tseng, Y.; Cheng, F.; Yeh, C. Near-Infrared Light-Responsive Intracellular Drug and siRNA Release Using Au Nanoensembles with Oligonucleotide-Capped Silica Shell. *Adv. Mater.* **2012**, *24*, 3309−3314.

DOI: 10.1021/acsami.6b13876
ACS Appl. Mater. Interfaces 2017, 9, 2123−2129

(9) Chen, Y.; Chen, H.; Zhang, S.; Chen, F.; Zhang, L.; Zhang, J.; Zhu, M.; Wu, H.; Guo, L.; Feng, J.; Shi, J. Multifunctional Mesoporous Nanoellipsoids for Biological Bimodal Imaging and Magnetically Targeted Delivery of Anticancer Drugs. *Adv. Funct. Mater.* **2011**, *21*, 270−278.
(10) Wu, H.; Zhang, S.; Zhang, J.; Liu, G.; Shi, J.; Zhang, L.; Cui, X.; Ruan, M.; He, Q.; Bu, W. A Hollow-Core, Magnetic, and Mesoporous Double Shell Nanostructure: In Situ Decomposition/Reduction Synthesis, Bioimaging, and Drug-Delivery Properties. *Adv. Funct. Mater.* **2011**, *21*, 1850−1862.
(11) Li, L.; Tang, F.; Liu, H.; Liu, T.; Hao, N.; Chen, D.; Teng, X.; He, J. In Vivo Delivery of Silica Nanorattle Encapsulated Docetaxel for Liver Cancer Therapy with Low Toxicity and High Efficacy. *ACS Nano* **2010**, *4*, 6874−6882.
(12) Li, L.; Guan, Y.; Liu, H.; Hao, N.; Liu, T.; Meng, X.; Fu, C.; Li, Y.; Qu, Q.; Zhang, Y.; Ji, S.; Chen, L.; Chen, D.; Tang, F. Silica Nanorattle Doxorubicin Anchored Mesenchymal Stem Cells for Tumor-Tropic Therapy. *ACS Nano* **2011**, *5*, 7462−7470.
(13) Wang, H.; Lee, D. K.; Chen, K. Y.; Chen, J. Y.; Zhang, K.; Silva, A.; Ho, C. M.; Ho, D. Mechanism-Independent Optimization of Combinatorial Nanodiamond and Unmodified Drug Delivery Using a Phenotypically Driven Platform Technology. *ACS Nano* **2015**, *9*, 3332−3344.
(14) Zhang, Y.; Cui, Z.; Kong, H.; Xia, K.; Pan, L.; Li, J.; Sun, Y.; Shi, J.; Wang, L.; Zhu, Y.; Fan, C. One-Shot Immunomodulatory Nanodiamond Agents for Cancer Immunotherapy. *Adv. Mater.* **2016**, *28*, 2699−2708.
(15) Lai, J.; Shah, B. P.; Garfunkel, E.; Lee, K. Versatile Fluorescence Resonance Energy Transfer-Based Mesoporous Silica Nanoparticles for Real-Time Monitoring of Drug Release. *ACS Nano* **2013**, *7*, 2741−2750.
(16) Mackowiak, S. A.; Schmidt, A.; Weiss, V.; Argyo, C.; von Schirnding, C.; Bein, T.; Brauchle, C. Targeted Drug Delivery in Cancer Cells with Red-Light Photoactivated Mesoporous Silica Nanoparticles. *Nano Lett.* **2013**, *13*, 2576−2583.
(17) Solberg, S.; Landry, C. C. Adsorption of DNA into Mesoporous Silica. *J. Phys. Chem. B* **2006**, *110*, 15261−15268.
(18) Wu, S.; Hung, Y.; Mou, C. Compartmentalized Hollow Silica Nanospheres Templated from Nanoemulsions. *Chem. Mater.* **2013**, *25*, 352−364.
(19) Tang, F.; Li, L.; Chen, D. Mesoporous Silica Nanoparticles: Synthesis, Biocompatibility and Drug Delivery. *Adv. Mater.* **2012**, *24*, 1504−1534.
(20) Yang, J.; Lee, J.; Kang, J.; Lee, K.; Suh, J.; Yoon, H.; Huh, Y.; Haam, S. Hollow Silica Nanocontainers as Drug Delivery Vehicles. *Langmuir* **2008**, *24*, 3417−3421.
(21) Du, X.; He, J. Spherical Silica Micro/Nanomaterials with Hierarchical Structures: Synthesis and Applications. *Nanoscale* **2011**, *3*, 3984−4002.
(22) Lou, X.; Archer, L. A.; Yang, Z. Hollow Micro-/Nanostructures: Synthesis and Applications. *Adv. Mater.* **2008**, *20*, 3987−4019.
(23) Wu, X.; Xu, D. Formation of Yolk/SiO_2 Shell Structures Using Surfactant Mixtures as Template. *J. Am. Chem. Soc.* **2009**, *131*, 2774−2775.
(24) Zhu, G.; Qiu, S.; Terasaki, O.; Wei, Y. Polystyrene Bead-Assisted Self-Assembly of Microstructured Silica Hollow Spheres in Highly Alkaline Media. *J. Am. Chem. Soc.* **2001**, *123*, 7723−7724.
(25) Ziegler, C.; Eychmuller, A. Seeded Growth Synthesis of Uniform Gold Nanoparticles with Diameters of 15−300 nm. *J. Phys. Chem. C* **2011**, *115*, 4502−4506.
(26) Zhang, S.; Xu, L.; Liu, H.; Zhao, Y.; Zhang, Y.; Wang, Q.; Yu, Z.; Liu, Z. A Dual Template Method for Synthesizing Hollow Silica Spheres with Mesoporous Shells. *Mater. Lett.* **2009**, *63*, 258−259.
(27) Jana, N. R.; Gearheart, L.; Murphy, C. J. Seeding Growth for Size Control of 5−40 nm Diameter Gold Nanoparticles. *Langmuir* **2001**, *17*, 6782−6786.
(28) Gorelikov, I.; Matsuura, N. Single-Step Coating of Mesoporous Silica on Cetyltrimethyl Ammonium Bromide-Capped Nanoparticles. *Nano Lett.* **2008**, *8*, 369−373.
(29) Li, N.; Yu, Z.; Pan, W.; Han, Y.; Zhang, T.; Tang, B. A Near-Infrared Light-Triggered Nanocarrier with Reversible DNA Valves for Intracellular Controlled Release. *Adv. Funct. Mater.* **2013**, *23*, 2255−2262.
(30) Kim, J.; Kim, H. S.; Lee, N.; Kim, T.; Kim, H.; Yu, T.; Song, I. C.; Moon, W. K.; Hyeon, T. Multifunctional Uniform Nanoparticles Composed of a Magnetite Nanocrystal Core and a Mesoporous Silica Shell for Magnetic Resonance and Fluorescence Imaging and for Drug Delivery. *Angew. Chem., Int. Ed.* **2008**, *47*, 8438−8441.
(31) Yu, Z.; Li, N.; Zheng, P.; Pan, W.; Tang, B. Temperature-Responsive DNA-Gated Nanocarriers for Intracellular Controlled Release. *Chem. Commun.* **2014**, *50*, 3494−3497.
(32) Li, N.; Chang, C.; Pan, W.; Tang, B. A Multicolor Nanoprobe for Detection and Imaging of Tumor-Related mRNAs in Living Cells. *Angew. Chem., Int. Ed.* **2012**, *51*, 7426−7430.
(33) Tan, B.; Rankin, S. E. Dual Latex/Surfactant Templating of Hollow Spherical Silica Particles with Ordered Mesoporous Shells. *Langmuir* **2005**, *21*, 8180−8187.
(34) Hao, N.; Jayawardana, K. W.; Chen, X.; Yan, M. One-Step Synthesis of Amine-Functionalized Hollow Mesoporous Silica Nanoparticles as Efficient Antibacterial and Anticancer Materials. *ACS Appl. Mater. Interfaces* **2015**, *7*, 1040−1045.
(35) Siepmann, J.; Peppas, N. A. Higuchi Equation: Derivation, Applications, Use and Misuse. *Int. J. Pharm.* **2011**, *418*, 6−12.
(36) Andersson, J.; Rosenholm, J.; Areva, S.; Lindén, M. Influences of Material Characteristics on Ibuprofen Drug Loading and Release Profiles from Ordered Micro- and Mesoporous Silica Matrices. *Chem. Mater.* **2004**, *16*, 4160−4167.

DOI: 10.1021/acsami.6b13876
ACS Appl. Mater. Interfaces 2017, 9, 2123−2129